Received: 9 June 2022 | Revised: 28 October 2022 | Accepted: 2 November 2022

DOI: 10.1002/alz.12890

Alzheimer's & Dementia®
THE JOURNAL OF THE ALZHEIMER'S ASSOCIATION

FEATURED ARTICLE

Presynaptic membrane protein dysfunction occurs prior to neurodegeneration and predicts faster cognitive decline

Guoyu Lan[1,2] | **Anqi Li**[1] | **Zhen Liu**[1] | **Shaohua Ma**[2] | **Tengfei Guo**[1,3] | **for the Alzheimer's Disease Neuroimaging Initiative***

[1]Institute of Biomedical Engineering, Shenzhen Bay Laboratory, Shenzhen, China

[2]Tsinghua Shenzhen International Graduate School (SIGS), Tsinghua University, Shenzhen, China

[3]Institute of Biomedical Engineering, Peking University Shenzhen Graduate School, Shenzhen, China

Correspondence
Tengfei Guo, Institute of Biomedical Engineering, Shenzhen Bay Laboratory, No.5 Kelian Road, Shenzhen, 518132, China.
Email: tengfei.guo@pku.edu.cn

*Data used in preparation of this article were obtained from the Alzheimer's Disease Neuroimaging Initiative (ADNI) database (adni.loni.usc.edu). As such, the investigators within the ADNI contributed to the design and implementation of ADNI and/or provided data but did not participate in analysis or writing of this report. A complete listing of ADNI investigators can be found at: http://adni.loni.usc.edu/wp-content/uploads/how_to_apply/ADNI_Acknowledgement_List.pdf

Funding information
National Natural Science Foundation of China, Grant/Award Number: 82171197; Shenzhen Bay Laboratory Key Project, Grant/Award Number: S211101002-2; Shenzhen Bay Laboratory Open Project, Grant/Award Number: SZBL2020090501014

Abstract

Introduction: Although presynaptic loss measured by cerebrospinal fluid (CSF) growth-associated protein-43 (GAP-43) is significantly involved in Alzheimer's disease (AD), the sequential association between CSF GAP-43 and AD-typical neurodegeneration is poorly understood.

Methods: We compared baseline CSF GAP-43 levels (n = 730) and longitudinal CSF GAP-43 changes (n = 327) in various biological stages of AD, and investigated their relationships with cross-sectional and longitudinal measures of residual hippocampal volume, ^{18}F-fluorodeoxyglucose PET, regional gray matter volume and cortical thickness, and cognition.

Results: Elevated CSF GAP43 levels were significantly associated with faster rates of hippocampal atrophy, AD-signature hypometabolism and cortical thinning, and middle temporal gray matter atrophy-related and AD-signature hypometabolism-related cognitive decline. In contrast, baseline levels of all these neurodegeneration biomarkers did not predict longitudinal CSF GAP-43 increases.

Discussion: These findings suggest that presynaptic loss may occur prior to neurodegeneration, highlighting the importance of lowing tau aggregation and tau-related synaptic dysfunction in elderly adults and AD patients.

KEYWORDS
brain atrophy, cognitive decline, CSF GAP-43, hypometabolism, presynapse

1 | BACKGROUND

In various neurodegenerative diseases, including Alzheimer's disease (AD)[1,2], progressive synaptic dysfunction is the fundamental neuropathology highly linked to neuronal death. Previous studies[3–5] confirm that AD patients experience substantial synapse loss in several brain locations, including the hippocampal dental gyrus and frontal and temporal cortex. Emerging evidence[6–10] from both animal models and human brains supports the synaptotoxic role of abnormal aggregation of soluble β-amyloid (Aβ) and phosphorylated tau (p-Tau), as well as glia-mediated neuroinflammation, even though the molecular mechanism underlying synaptic degeneration in AD is not fully understood.

Synaptic loss substantially correlates with downstream cognitive impairment,[10,11] and previous studies found that presynaptic proteins appear to be damaged more than the

postsynaptic proteins in AD brains.[12–14] Growth-associated protein-43 (GAP-43) is a presynaptic membrane protein decreased in the frontal cortex and some hippocampal areas of postmortem AD brains.[15,16] Elevated cerebrospinal fluid (CSF) GAP-43 levels have been observed in both asymptomatic and symptomatic AD patients, reflecting a presynaptic dysfunction.[17–19] However, the sequential relationship between CSF GAP-43 and neurodegeneration is poorly characterized. According to a recent cross-sectional cohort investigation, CSF GAP-43 levels were positively associated with cortical glucose metabolism but negatively related to AD-signature cortical thickness in preclinical AD.[19] Although it is widely acknowledged that synaptic damage is a sign of neurodegeneration[11], little is known about how it relates to brain atrophy, cortical thinning, hypometabolism, and cognitive decline or whether it is a cause or a consequence of these biomarkers of neurodegeneration.

In the present study, we investigated the dynamic changes in CSF GAP-43 among different A/T/N profiles and their association with neuroimaging biomarkers of neurodegeneration and cognitive decline using cross-sectional and longitudinal data from the Alzheimer's Disease Neuroimaging Initiative (ADNI) cohort. The main objectives are to determine (1) the alteration of CSF GAP-43 among different biological stages of AD, (2) the association between CSF GAP-43 and neurodegeneration, and (3) the interaction effect of CSF GAP-43 with neurodegeneration on cognitive decline. We hypothesize that presynaptic loss, as measured by CSF GAP-43, precedes neurodegeneration and predicts more rapid cognitive decline at a given level of neurodegeneration. This study may help to advance our understanding of the neuropathology of presynaptic loss in neurodegenerative diseases.

RESEARCH IN CONTEXT

1. **Systematic review**: Literature reviews in PubMed and Google Scholar suggest cerebrospinal fluid (CSF) growth-associated protein-43 (GAP-43) is significantly involved in Alzheimer's disease (AD), but the sequential association between CSF GAP-43 and neurodegeneration has been poorly investigated.
2. **Interpretation**: CSF GAP-43 increases were significantly related to abnormal tau pathology rather than cortical Aβ plaques and neurodegeneration. Elevated CSF GAP-43 was associated with more rapid hippocampal atrophy, cortical thinning, hypometabolism, and cognitive decline, whereas baseline levels of these neurodegeneration biomarkers did not predict longitudinal changes in CSF GAP-43. Higher CSF GAP-43 concentrations predicted further faster cognitive decline in addition to neurodegeneration. These findings highlight the importance of lowing tau aggregation and tau-related synaptic dysfunction to maintain better brain structural and cognitive function in aging and AD patients.
3. **Future directions**: It would be helpful to validate these findings in other presynaptic or postsynaptic biomarkers based on independent cohorts.

2 | METHODS

2.1 | Participants

Data used in the preparation of this article were obtained from the ADNI database (adni.loni.usc.edu). The ADNI was launched in 2003 as a public-private partnership, led by Principal Investigator Michael W. Weiner, MD. The primary goal of ADNI has been to test whether serial magnetic resonance imaging (MRI), positron-emission tomography (PET), other biological markers, and clinical and neuropsychological assessment can be combined to measure the progression of mild cognitive impairment (MCI) and early AD. The ADNI study was approved by institutional review boards of all participating centers, and written informed consent was obtained from all participants or their authorized representatives.

This study included 730 participants (232 CU, 395 MCI, and 104 dementia) from the ADNI cohort. All participants had concurrent (within one year) baseline ^{18}F-florbetapir (FBP) Aβ PET, CSF p-Tau$_{181}$, CSF GAP-43, and ^{18}F-fluorodeoxyglucose (FDG) PET, as well as longitudinal structure MRI and cognitive assessments. Among them, 377 individuals had longitudinal FDG PET, and 327 individuals had simultaneous longitudinal Aβ PET, CSF p-Tau$_{181}$, and CSF GAP-43 data.

2.2 | CSF biomarkers

CSF GAP-43 was measured at the Clinical Neurochemistry Laboratory of the Sahlgrenska University Hospital (Mölndal, Sweden) using an in-house ELISA as described previously.[17] Linear mixed effect (LME) models were used to calculate slopes of CSF GAP-43 for all the participants with longitudinal CSF GAP-43 data, adjusting for age and sex and including a random slope and intercept. CSF p-Tau$_{181}$ was analyzed by the ADNI biomarker core group using the fully automated Roche Elecsys.[20] The threshold to define abnormal CSF p-Tau$_{181}$ (T+) was ≥ 23 pg/ml as described in the Supplementary Materials (Figure S1-2).

2.3 | PET and MRI imaging processing

FBP PET and FDG PET data were acquired from 50 to 70 min (FBP, 4 to 5-min frames) and 30 to 60 min (FDG, 6 to 5-min frames) post-injection. PET images were motion corrected, time-averaged, and summed into one static frame, and more details are given elsewhere (http://adni-info.org).

Cortical florbetapir uptakes in 68 regions of interest (ROIs) defined by the Desikan-Killiany atlas[21] were extracted using FreeSurfer (V7.1.1) from each FBP PET scan that coregistered to the individual corresponding structural MRI scan. A COMPOSITE standardized uptake value ratio (SUVR) was calculated by referring florbetapir

uptake in AD summarized cortical regions (including frontal, cingulate, parietal, and temporal areas) to the mean uptake of the whole cerebellum.[22] The positivity of COMPOSITE FBP SUVR (A+) was defined as SUVR ≥ 1.11.[22]

For FDG PET images, we first coregistered each FDG PET scan to the MNI PET template and subsequently completed spatial normalization to transfer FDG PET images to MNI space in SPM12. FDG SUVR in a pre-defined MetaROIs were calculated by normalizing averaged FDG counts in MetaROIs to that found in the upper 50% of voxels in a pons/vermis reference region[23] based on the spatial normalized FDG PET image. Slopes of MetaROIs FDG SUVR were calculated for all the participants with longitudinal FDG PET data using LME models, adjusting for age and sex and including a random slope and intercept. The positivity of MetaROIs FDG SUVR (N+) was defined as SUVR ≤ 1.19 as described in the Supplementary Materials (Figure S3-4).

68 FreeSurfer-defined gray matter volumes (GMV) and cortical thicknesses, and hippocampal volume (HCV) were calculated from the structural MRI scan via FreeSurfer. Bilateral HCV was adjusted by the estimated intracranial volume.[24] The residual HCV (rHCV) was calculated as the difference between the raw and expected HCV as we described previously.[25] Temporal-MetaROI cortical thickness was computed as a surface-area weighted average of the mean cortical thickness in the entorhinal, fusiform, inferior temporal, and middle temporal cortices.[26] Slopes of rHCV, temporal-MetaROI cortical thickness, and GMV and cortical thicknesses of 68 ROIs were calculated for all the participants with longitudinal MRI data using LME models, adjusting for age and sex, and including a random slope and intercept. The cutoff value to define rHCV positivity (N+) was ≤ -0.67 $cm^{3,}$ as described in the Supplementary material (Figure S5-6).

2.4 | Biological stages defined by A/T/N biomarkers

Participants were classified into different A/T/N profiles according to the abnormal status of Aβ PET (A ±), CSF p-Tau_{181} (T ±), and rHCV or MetaROIs FDG SUVR (N ±) defined by the cutoff values as described above. For sensitivity analysis, we also used alternative cutoff values for CSF p-Tau_{181} ≥ 19.2 pg/ml[27], rHCV ≤ -0.70 cm^3[24,28], and MetaROIs FDG SUVR ≤ 1.41[26] reported by different cohorts to define T ± and N ± .

2.5 | Cognitive assessments

Previously validated preclinical Alzheimer cognitive composite (PACC)[29] scores were used to represent global cognition, the details of calculating PACC scores in ADNI can be found in our previous report.[25] Slopes of PACC scores were calculated for all the participants with longitudinal PACC data using LME models, adjusting for age, sex, and education, and including a random slope and intercept.

2.6 | Statistical analysis

All statistical analyses were conducted in R version 4.1.1 (The R Foundation for Statistical Computing). Data were presented as median (interquartile range [IQR]) or number (%) unless otherwise noted. The demographics and clinical characteristics between the CU and cognitively impaired (CI) groups were compared using a two-tailed Mann-Whitney U test or Fisher's exact test at a significance level of $p < 0.05$ unless otherwise noted.

Generalized linear models (GLM) were used to compare cross-sectional, and longitudinal CSF GAP-43 changes among different A/T/N groups, controlling for age, sex, education, and *APOE-ε4* status. A false discovery rate (FDR) of 0.05 was applied using the Benjamini-Hochberg approach for multiple comparisons correction.

To determine the sequential relation between CSF GAP-43 and neurodegeneration, we used the GLM model to investigate the cross-sectional and longitudinal associations of CSF GAP-43 with the most commonly-used AD neurodegeneration biomarkers, including rHCV, temporal-MetaROI cortical thickness, and MetaROIs FDG SUVR, and controlling for the same covariates above. Additionally, we explored the strongest cortical region with CSF GAP-43 by examining the associations of baseline CSF GAP-43 with the slopes of GMV and cortical thickness in 68 FreeSurfer-defined ROIs. Benjamini-Hochberg approach was used for multiple comparisons correction (FDR < 0.05) across 68 ROIs. Conversely, we also investigated whether baseline GMV and cortical thickness in the strongest cortical region can predict longitudinal CSF GAP-43 increases over time, controlling for the same covariates above.

Finally, we investigated the interaction effect of baseline CSF GAP-43 with rHCV, temporal-MetaROI cortical thickness, MetaROIs FDG SUVR, and middle temporal GMV and cortical thickness on the longitudinal changes of PACC scores, controlling for the same covariates above. Furthermore, receiver operating characteristic (ROC) analysis was performed to ascertain whether baseline CSF GAP-43 can predict the conversion from MCI to dementia by including or removing *APOE-ε4*, Aβ PET, or CSF p-Tau_{181} from the models.

3 | RESULTS

3.1 | Demographics

Table 1 summarized the clinical characteristics at baseline of participants. Among 730 participants, 347 (48%) were females, 333 (46%) were *APOE-ε4* carriers, 392 (54%) were Aβ positive, and the medians (IQR) of age and education were 72.6 (10.3) and 16 (4), respectively. Longitudinal data of structure MRI, PACC scores, FDG PET, and CSF GAP-43 were also illustrated in Table 1. There was no difference in age between the CU and CI groups. However, CI individuals had higher *APOE4* prevalence ($p < 0.001$), lower percentage of females ($p < 0.01$), and lower education ($p < 0.01$) than CU individuals.

TABLE 1 Demographics of participants in CU and CI groups

Characteristic	CU ($n = 232$)	CI ($n = 498$)
Age, years	72.6 (9.0)	72.4 (10.9)
Female, No. (%)	128 (55)	219 (44) [b]
Education, years	16.5 (2.0)	16.0 (4.0) [b]
APOE-ε4 carriers, No. (%)	66 (28)	267 (54) [a]
Aβ PET, SUVR	1.06 (0.19)	1.25 (0.42) [a]
CSF p-Tau$_{181}$, pg/ml	19.2 (10.8)	25.0 (18.6) [a]
CSF GAP-43, pg/ml	4254 (3217)	4549 (3343) [c]
rHCV, cm^3	-0.04 (0.49)	-0.34 (0.69) [a]
Temporal-ROI cortical thickness, mm	2.70 (0.12)	2.64 (0.20) [a]
MetaROIs FDG PET, SUVR	1.30 (0.15)	1.20 (0.21) [a]
PACC scores	0.43 (3.54)	-6.23 (9.11) [a]
Longitudinal MRI and PACC data		
Visits of MRI, median (IQR, Range)	4 (2, 2 - 9)	4 (1, 2 - 12)
Duration of MRI, years, median (IQR, Range)	2.3 (4.7, 0.2 - 10.1)	1.3 (3.0, 0.2 - 11.2)
Visits of PACC, median (IQR, Range)	5 (3, 2 - 10)	5 (4, 2 - 13)
Duration of PACC, years, median (IQR, Range)	6.0 (4.7, 0.5 - 10.5)	3.5 (3.7, 0.4 - 11.2)
377 participants with longitudinal FDG PET imaging	$n = 111$	$n = 266$
Visits of FDG PET, median (IQR, Range)	2 (0, 2 - 3)	2 (0, 2 - 3)
Duration of FDG PET, years, median (IQR, Range)	2.0 (0.1, 1,5 - 7.1)	2.0 (3.3, 0.8 - 9.2)
327 participants with longitudinal CSF GAP43	$n = 127$	$n = 200$
Visits of CSF GAP43, median (IQR, Range)	2 (1, 2 - 3)	2 (1, 2 - 4)
Duration of CSF GAP43, years, median (IQR, Range)	2.1 (2.0, 1.3 - 5.0)	2.1 (2.0, 1.7 - 6.0)

Note: Data are presented as median (M) and interquartile range (IQR) or participant's number (n) and percentage (%). Data were compared using a two-tailed Mann-Whitney U test or Fisher's exact test.

Abbreviations: APOE, apolipoprotein E; CI, cognitively impaired; CSF, cerebrospinal fluid; CU, cognitively unimpaired; FDG, fluorodeoxyglucose; GAP-43, growth-associated protein-43; HCV, hippocampus volume; IQR, interquartile range; PACC, Preclinical Alzheimer Cognitive Composite; PET, positron emission computed tomography; p-Tau$_{181}$, phosphorylated tau 181; SUVR, standard uptake value ratio.

[a] $p < 0.001$ versus CU.

[b] $p < 0.01$ versus CU.

[c] $p < 0.05$ versus CU.

3.2 | Comparisons of CSF GAP-43 among different biological stages

To explore the association of CSF GAP-43 with AD-core pathologies and neurodegeneration, we compared cross-sectional and longitudinal CSF GAP-43 changes among different A/T/N profiles. When the neurodegeneration (N ±) was defined by hippocampal atrophy (rHCV), the A-/T+/N-, A-/T+/N+, A+/T+/N-, and A+/T+/N+ individuals but not the A-/T-/N+, A+/T-/N-, and A+/T-/N+ individuals had higher CSF GAP-43 concentrations and faster rates of increases in CSF GAP-43 compared to the A-/T-/N- individuals, regardless of Aβ positivity and hippocampal atrophy (Figure 1A-B and Table S1). For comparison purposes, we repeated the analyses using AD-signature hypometabolism (MetaROIs FDG SUVR) as the biomarker of neurodegeneration and found similar results (Figure 1C-D and Table S2). Notably, no significant difference was found in CSF GAP-43 concentrations and longitudinal CSF GAP-43 changes among A-/T+/N-, A-/T+/N+, A+/T+/N- and A+/T+/N+ individuals or among A-/T-/N-, A-/T-/N+, A+/T-/N- and A+/T-/N+ individuals when either rHCV or FDG PET defined the neurodegeneration (N ±).

Additionally, these findings were substantially the same as those obtained when we used the alternative cutoffs of CSF p-Tau$_{181}$, rHCV, and MetaROIs FDG SUVR to define T ± and N ± (Figure S7).

3.3 | Association of CSF GAP-43 with hippocampal atrophy, cortical thinning, and hypometabolism

At baseline, CSF GAP-43 concentrations were negatively associated with rHCV (standardized β (β_{std}) = -0.08 [95% confidence interval (CI), -0.16 to 0.01], $p = 0.025$), but not related to temporal-MetaROI cortical thickness (β_{std} = 0.005 [95% CI, -0.07 to 0.08], $p = 0.894$) and MetaROIs FDG SUVR (β_{std} = -0.06 [95% CI, -0.13 to 0.01], $p = 0.082$) in the whole cohort (Figure S8). Longitudinally, higher baseline CSF GAP-43 concentrations were related to faster rates of decreases in rHCV (β_{std} = -0.13 [95% CI, -0.20 to -0.06], $p < 0.001$) and temporal-MetaROI cortical thickness (β_{std} = -0.15 [95% CI, -0.22 to -0.08], $p < 0.001$) (Figure 2A-B). Among 377 individuals with longitudinal FDG PET images, higher baseline CSF GAP-43 concentrations were also associated with faster rates of decrease in MetaROIs FDG SUVR (β_{std} = -0.17 [95% CI, -0.27 to -0.07], $p < 0.001$) (Figure 2C). After stratified by cognitive status, the negative associations of baseline CSF GAP-43 with slopes of rHCV, temporal-MetaROI cortical thickness, and MetaROIs FDG SUVR were retained only in CI individuals but not in CU individuals (Table S3). In contrast, the baseline levels of rHCV, temporal-MetaROI cortical thickness, and MetaROIs FDG SUVR did not predict longitudinal increases in CSF GAP-43 among 327 individuals with longitudinal CSF GAP-43 measurements, either in the whole cohort (Figure 2D-F) or in each subgroup (Figure S9).

3.4 | Association of CSF GAP-43 with regional GMV and cortical thickness

In the whole cohort, across 68 FreeSurfer-defined brain regions, baseline CSF GAP-43 concentrations were negatively related to faster rates of decrease in GMV in 28 regions (Figure 3A and Table S4) and cortical thickness in 40 regions (Figure 3B and Table S5). The strongest negative associations with slopes of GMV (β_{std} = -0.17 [95% CI, -0.24 to -0.10], $p < 0.001$) and cortical thickness (β_{std} = -0.17 [95% CI, -0.25 to -0.10], $p < 0.001$) were found in the middle temporal region

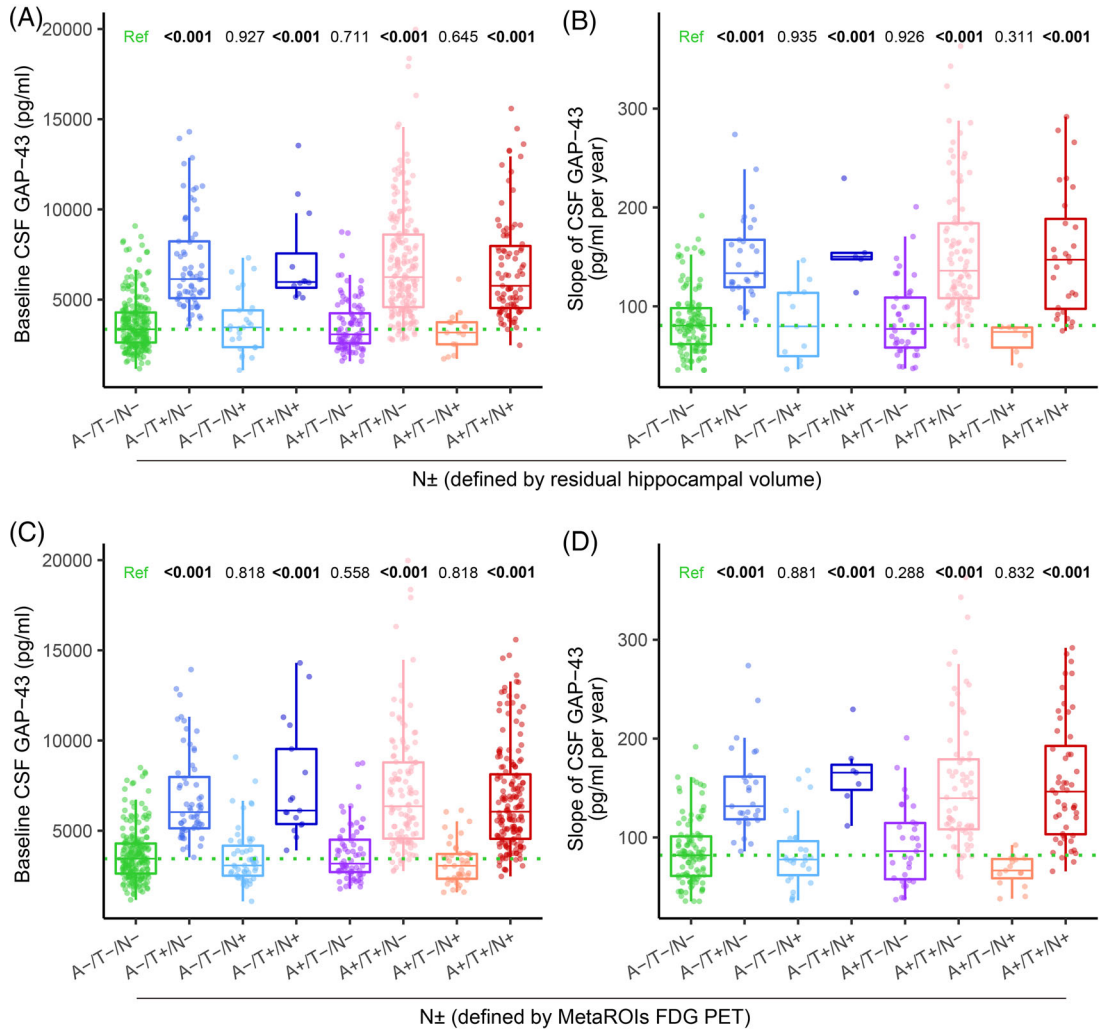

FIGURE 1 Comparison of cross-sectional and longitudinal CSF GAP-43 among different biological stages. Comparison of baseline CSF GAP-43 (A) and slope of CSF GAP-43 (B) among different A/T/N groups (N ± was defined by rHCV). Comparison of baseline CSF GAP-43 (C) and slope of CSF GAP-43 (D) among different A/T/N groups (N ± was defined by MetaROIs FDG PET). The boxplots depict the median (horizontal bar), interquartile range (IQR, hinges), and 1.5 × IQR (whiskers). Each point represents an individual, and green dashed lines represent the median values of the reference. The p values of the comparisons with the reference (Ref) are shown at the top of the bar, adjusting for age, sex, education, and APOE-ε4 status

(Figure 3C-D), and these associations remained significant in CI individuals but not in CU individuals (Table S6). Conversely, the baseline levels of GMV and cortical thickness in the middle temporal region were unrelated to longitudinal changes in CSF GAP-43 (Figure 3E-F). Notably, no positive association was observed between baseline CSF GAP-43 and slopes of GMV and cortical thickness in 68 cortical regions.

3.5 | Interaction of CSF GAP-43 with neurodegeneration on cognitive decline

In the whole cohort, higher baseline CSF GAP-43 concentrations were related to faster rates of decreases in PACC scores (β_{std} = -0.18 [95% CI, -0.24 to -0.11], $p < 0.001$). Moreover, we tested whether CSF GAP-43 had an interaction effect with the above neuroimaging biomarkers in predicting longitudinal cognitive decline. Importantly, we found that baseline CSF GAP-43 significantly interacted with baseline and longitudinal metaROIs FDG SUVR and middle temporal GMV in predicting longitudinal cognitive decline (Table 2), showing that individuals with high CSF GAP-43 levels had more pronounced positive associations of metaROIs FDG SUVR and middle temporal GMV with slopes of PACC scores than individuals with low CSF GAP-43 levels (Figure. 4). However, no significant interaction between baseline CSF GAP-43 and other neurodegeneration biomarkers (rHCV, temporal-MetaROI or middle temporal cortical thickness) was observed in predicting longitudinal cognitive decline (Figure S10 and Table S7).

Last, among 355 individuals who were MCI at baseline, we found that 115 individuals progressed to dementia at a median (IQR) follow-up of 4.0 (4.0) years. Baseline CSF GAP-43 concentrations were

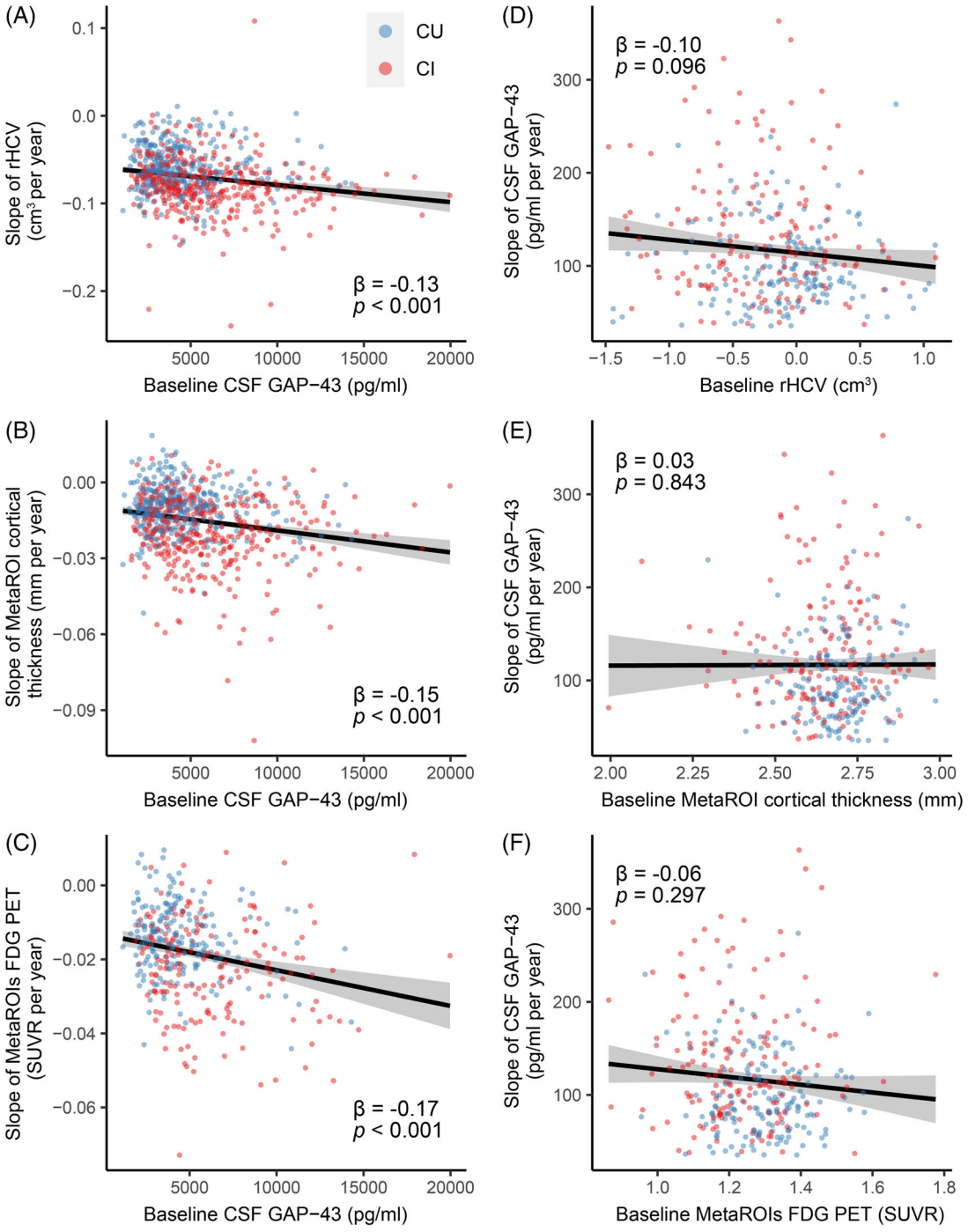

FIGURE 2 Association of CSF GAP-43 with hippocampal atrophy, MetaROIs cortical thickness, and hypometabolism. Prediction of longitudinal changes of rHCV (A), temporal-MetaROI cortical thickness (B), and MetaROIs FDG PET (C) by baseline CSF GAP-43. Association of baseline rHCV (D), temporal-MetaROI cortical thickness (E), and MetaROIs FDG PET (F) with the slope of CSF GAP-43. The points (blue, CU; red, CI) and solid lines represent the individuals and regression lines, respectively. The standardized regression coefficients (β) and p values were computed using a linear model across all participants, adjusting for age, sex, education, and APOE-ε4 status

significantly increased in those who subsequently developed dementia than in those who were stable MCI at follow-up (Figure S11). Furthermore, CSF GAP-43 concentrations predicted the conversion from MCI to dementia with an AUC of 0.66 (Figure 5A). When combing CSF GAP-43 with *APOE-ε4*, Aβ PET, and CSF p-Tau$_{181}$, the ROC analysis showed the most excellent AUC of 0.79 for the prediction.

4 | DISCUSSION

In the current study, we investigated baseline and longitudinal alternations in CSF GAP-43 between different biological stages of AD and how they relate to hippocampal atrophy, cortical thinning, hypometabolism, and cognitive decline cross-sectionally and longitudinally. Regardless

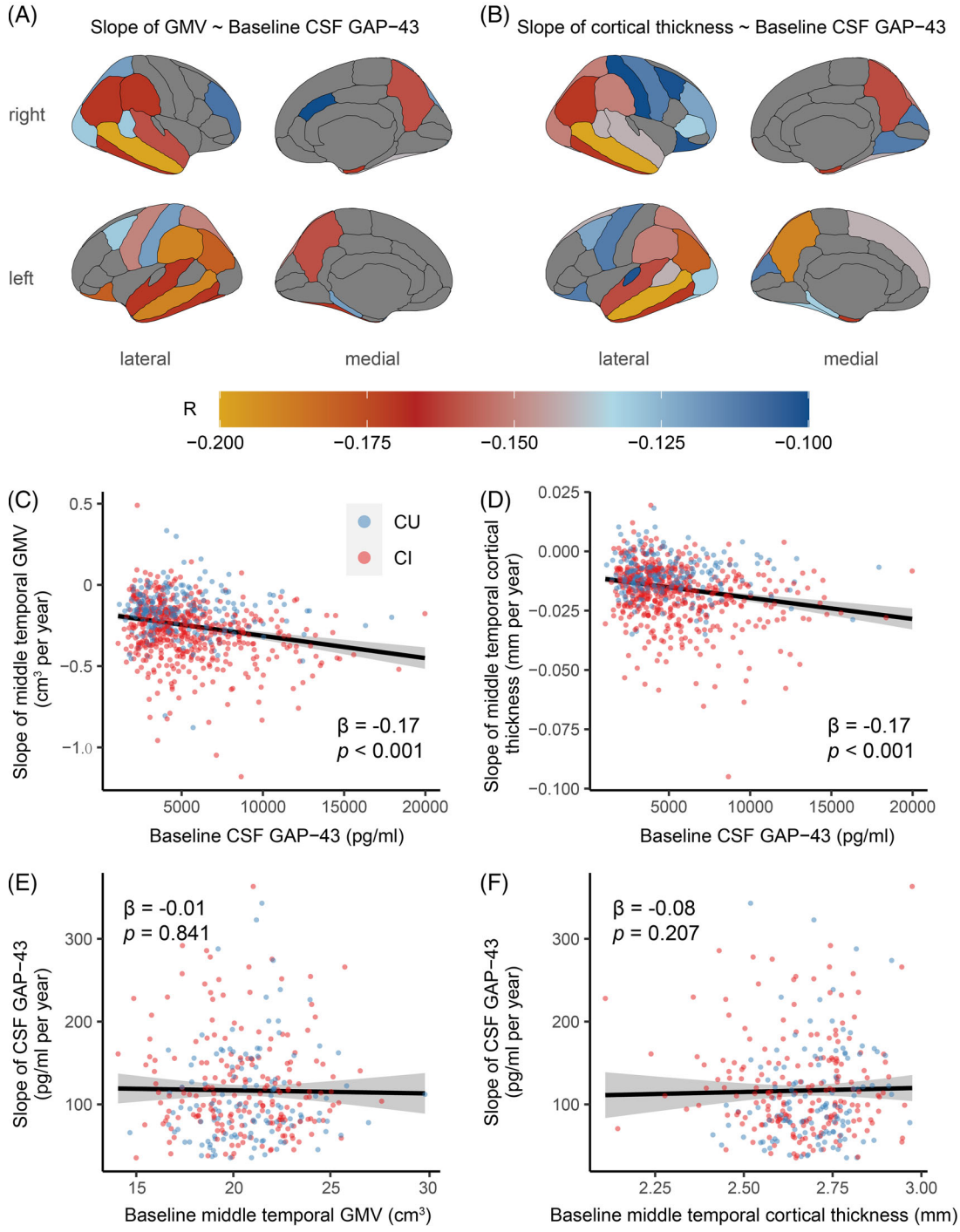

FIGURE 3 Association of CSF GAP-43 with regional GMV and cortical thickness correlation coefficients of baseline CSF GAP-43 with the slope of GMV (A) and cortical thickness (B) in brain map. Association of baseline CSF GAP-43 with the slope of GMV (C) and cortical thickness (D) in middle temporal. Association of baseline GMV (E) and cortical thickness (F) in middle temporal with the slope of CSF GAP-43. The points (blue, CU; red, CI) and solid lines represent the individuals and regression lines, respectively. The standardized regression coefficients (β) and p values were computed using a linear model across all participants, adjusting for age, sex, education, and APOE-ε4 status

of amyloid positivity, hippocampal atrophy, and hypometabolism, we found that individuals with abnormal tau pathology had higher CSF GAP-43 concentrations and faster rates of CSF GAP-43 increases than those without significant tau pathology. Furthermore, higher baseline CSF GAP-43 concentrations were related to more rapid brain atrophy, cortical thinning, and hypometabolism over time. In contrast, longitudinal changes in CSF GAP-43 could not be predicted by the baseline levels of those neuroimaging biomarkers, implying that CSF GAP-43 increases may be an earlier event than neurodegeneration measured by FDG PET or structural MRI. Together with the previous

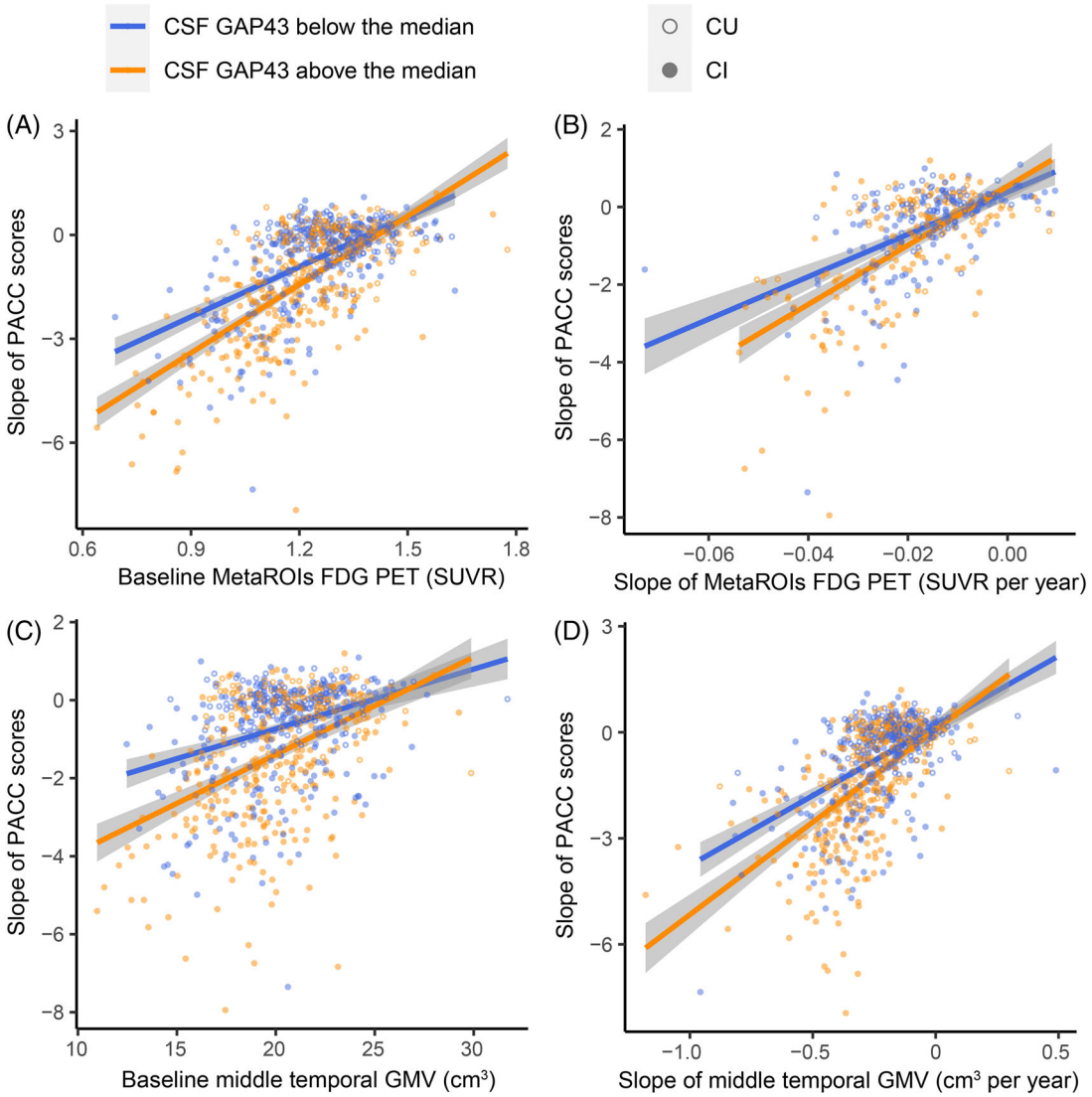

FIGURE 4 Interaction of CSF GAP-43 with neurodegeneration on cognitive decline. Baseline CSF GAP-43 significantly modified the association of cross-sectional and longitudinal MetaROIs FDG PET (A-B) and middle temporal GMV (C-D) with slopes of PACC scores. The points (blue, individuals with CSF GAP43 concentrations below the median; orange, individuals with CSF GAP43 concentrations above the median) and solid lines represent the individuals and regression lines, respectively

studies[30–34], one hypothetical cascade model of AD may be concluded (Figure 5B). Last, we found that baseline CSF GAP-43 concentrations had a modulatory effect on the associations of AD-signature hypometabolism and middle temporal gray matter atrophy with longitudinal cognitive decline. These findings provide a novel insight into the interpretation of presynaptic loss measured by CSF GAP-43 preceding neurodegeneration. CSF GAP-43 may be a promising biomarker for tracking the disease progression in the absence of unequivocal neurodegeneration.

Previous cross-sectional studies[17–19,35,36] demonstrated that CSF GAP-43 concentrations were elevated in asymptomatic and symptomatic AD but not in suspected non-Alzheimer's disease pathophysiology. However, less is known about the changes in CSF GAP-43 in different biological stages of AD. In line with our findings, a recent study[37] reported increased CSF GAP-43 concentrations in MCI patients with tau pathology irrespective of CSF $A\beta_{42}$. Herein, we used A/T/N profiles to further extend the findings by indicating that both baseline and longitudinal CSF GAP-43 were explicitly elevated in the presence of tau pathology, supporting the determinant role of tau pathology in presynaptic loss measured by CSF GAP-43.[18,37] In contrast, amyloid plaques, hippocampal atrophy, and hypometabolism did not show an apparent influence on CSF GAP-43 increases. Notably, presynaptic protein GAP-43 plays an important role in synaptic plasticity and axonal regeneration[38,39], and its expression was induced by neuronal or axonal injury.[40] In this regard, GAP-43 increases may also reflect the mechanism underlying the repair of plasticity damages and effort to regenerative axonal sprouting, which is supposed to be explored by further study.

Recently, one observational study reported a negative association between CSF GAP-43 and AD-specific regional cortical thickness in

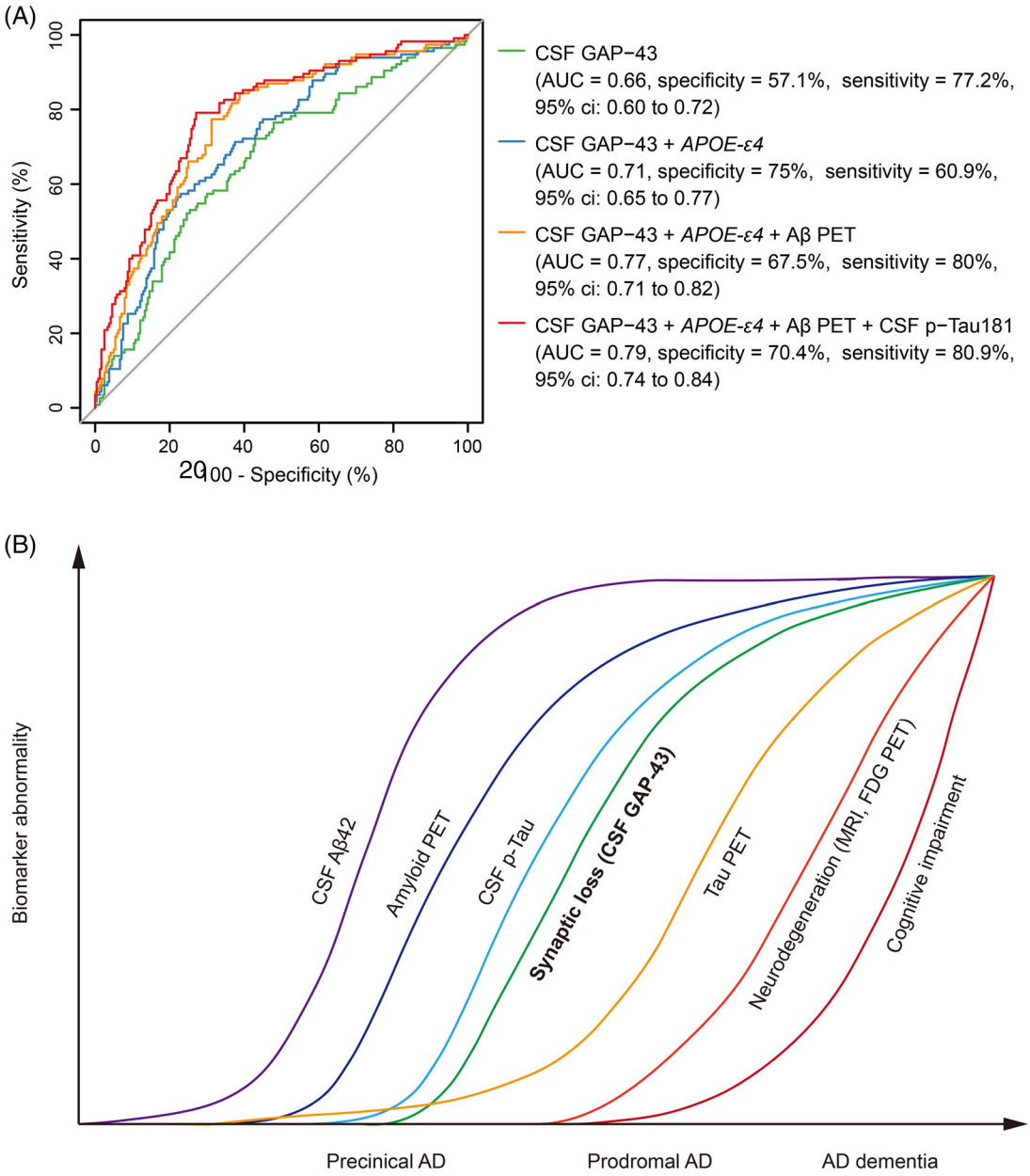

FIGURE 5 Prediction of the conversion to dementia. (A) ROC curves for baseline CSF GAP-43 combined with additional APOE-ε4, Aβ PET, and CSF p-Tau181 to predict the conversion from MCI to AD. (B) A model integrating the findings in this study, together with previous studies, depicts an approximative order of different CSF and imaging biomarkers in the AD continuum (Adapted from Dr. Clifford R. Jack Jr[34])

cognitively unimpaired individuals.[18] Given that synaptic loss and neurodegeneration are thought to constitute the major neuropathology leading to cognitive impairment in dementia[41–43], it is crucial to determine their sequential orders during disease progression. To this end, we explored the association between CSF GAP-43 and several commonly-used AD biomarkers of neurodegeneration, including hippocampal atrophy and AD-signature cortical thinning and hypometabolism. In a large cohort, our findings agree with the hypothesis that presynaptic loss, defined as elevated CSF GAP-43, occurs earlier than the neurodegeneration analyzed herein. Consistent with our findings, one observational study also showed that CSF synaptic protein changes were already present before the increases in CSF total-Tau, a marker of neurodegeneration, in preclinical AD.[44] Furthermore, an animal study revealed that synaptic loss and dysfunction were already detected in absence of hippocampal and entorhinal cortical atrophy[45], implying synaptic loss may precede brain atrophy at least in the tested regions. To further confirm our hypothesis, we explored the association of baseline CSF GAP-43 with longitudinal gray matter atrophy and cortical thinning across 68 cortical regions. The strongest negative association with CSF GAP-43 was found in the middle temporal region. Similarly, we did not observe the predictive effect of gray matter atrophy and cortical thinning at baseline on longitudinal CSF GAP-43 changes in

TABLE 2 The influence of CSF GAP-43 and neurodegeneration on longitudinal cognitive decline

Outcome variable: Slope of PACC scores	β_{std}	95% CI	*p* value
Main effect			
Baseline CSF GAP-43	-0.18	-0.24 to -0.11	< 0.001
Baseline MetaROIs FDG PET	0.60	0.55 to 0.66	< 0.001
Baseline middle temporal GMV	0.38	0.32 to 0.44	< 0.001
Slope of MetaROIs FDG PET	0.57	0.49 to 0.65	< 0.001
Slope of middle temporal GMV	0.53	0.47 to 0.59	< 0.001
Interaction with baseline CSF GAP-43			
Baseline MetaROIs FDG PET	0.21	0.10 to 0.32	< 0.001
Baseline middle temporal GMV	0.16	0.04 to 0.29	0.008
Slope of MetaROIs FDG PET	0.25	0.09 to 0.41	0.002
Slope of middle temporal GMV	0.17	0.05 to 0.28	0.005

Abbreviations: CI, confidence interval.; CSF, cerebrospinal fluid; FDG, fluorodeoxyglucose; GAP-43, growth-associated protein-43; PACC, Preclinical Alzheimer Cognitive Composite; PET, positron emission computed tomography.

any brain region. Together with our findings and previous literature, presynaptic loss measured by CSF GAP-43 may precede AD-typical neurodegeneration.

Consistent with our results, a previous study indicated that higher CSF GAP-43 concentrations were related to longitudinal declines in Mini-Mental State Examination (MMSE) scores over time.[17] Since our findings support that CSF GAP-43 alternations occur before apparent neurodegeneration, thus we investigated the modulatory effect of CSF GAP-43 on the association between neurodegeneration and cognitive decline. We found that individuals with higher CSF GAP-43 concentrations showed more pronounced AD-signature hypometabolism-associated and middle temporal gray matter atrophy-associated cognitive decline. This indicates that more presynaptic loss, likely to present earlier than brain atrophy and hypometabolism, is related to faster cognitive decline upon the same levels of neurodegeneration.[46,47] In addition, we also showed that CSF GAP-43, together with *APOE-ε4* and AD-core pathologies, significantly predicted the conversion from MCI to dementia, suggesting that CSF GAP-43 may be an additional measurement to predict longitudinal clinical progression.

Overall, this study tracked the dynamic of CSF GAP-43 among different biological stages of AD and explored the sequential association of CSF GAP-43 with brain structural and metabolic changes as well as their influence on cognitive decline in a large cohort. Our findings provide novel insights into the underlying mechanism and role of presynaptic loss in neurodegenerative diseases. However, several limitations should be considered in the current study. First, while the unidirectional predictive effect of CSF GAP-43 on neurodegeneration is well established herein, we cannot definitively conclude their causative association by one observational cohort. All we can confirm is that CSF GAP-43 increases may be predisposed to occur before neurodegeneration. Additionally, CSF GAP-43 is only an indirect biomarker of presynaptic loss, which cannot reflect the regional and structural damages to presynapse. Autopsy and neuroimaging examinations are needed to confirm these findings in the future. Finally, the association between other synaptic biomarkers (such as presynaptic SNAP-25[48] and synaptotagmin-1[49], and postsynaptic neurogranin[50]) and neurodegeneration still requires further investigation, as different synaptic proteins may reflect various aspects of synaptic dysfunction or loss occurring in the course of AD and other neurodegenerative dementia.

In summary, this study suggests that tau pathology instead of amyloid plaque parallels CSF GAP-43 increases reflecting presynaptic loss, which may occur prior to neurodegeneration and predict faster cognitive decline. These findings extend the understanding of the associations among AD pathology, presynaptic loss, neurodegeneration, and cognitive decline and highlight the importance of strategy targeting tau pathology at the early stage to diminish synaptic dysfunction and subsequent brain structural and cognitive impairments in AD and other neurodegenerative dementia. Crucially, CSF GAP-43 may be useful as an additional outcome biomarker to track the tau-related downstream event before the evident neurodegeneration.

ACKNOWLEDGMENTS

The authors thank all the ADNI participants and staff for their contributions to data acquisition. The Data collection and sharing for this project were funded by the Alzheimer's Disease Neuroimaging Initiative (ADNI) (National Institutes of Health Grant U01 AG024904) and DOD ADNI (Department of Defense award number W81XWH-12-2-0012). ADNI is funded by the National Institute on Aging, the National Institute of Biomedical Imaging and Bioengineering, and through generous contributions from the following: AbbVie, Alzheimer's Association; Alzheimer's Drug Discovery Foundation; Araclon Biotech; BioClinica, Inc.; Biogen; Bristol-Myers Squibb Company; CereSpir, Inc.; Eisai Inc.; Elan Pharmaceuticals, Inc.; Eli Lilly and Company; EuroImmun; F. Hoffmann-La Roche Ltd and its affiliated company Genentech, Inc.; Fujirebio; GE Healthcare; IXICO Ltd.; Janssen Alzheimer Immunotherapy Research & Development, LLC.; Johnson & Johnson Pharmaceutical Research & Development LLC.; Lumosity; Lundbeck; Merck & Co., Inc.; Meso Scale Diagnostics, LLC.; NeuroRx Research; Neurotrack Technologies; Novartis Pharmaceuticals Corporation; Pfizer Inc.; Piramal Imaging; Servier; Takeda Pharmaceutical Company; and Transition Therapeutics. The Canadian Institutes of Health Research is providing funds to support ADNI clinical sites in Canada. Private sector contributions are facilitated by the Foundation for the National Institutes of Health (www.fnih.org). The grantee organization is the Northern California Institute for Research and Education, and the study is coordinated by the Alzheimer's Disease Cooperative Study at the University of California, San Diego. ADNI

data are disseminated by the Laboratory for Neuro Imaging at the University of Southern California.

CONFLICT OF INTEREST

The authors declare no competing interests. Author disclosures are available in the supporting information.

ORCID

Tengfei Guo https://orcid.org/0000-0003-2982-0865

REFERENCES

1. Lepeta K, Lourenco MV, Schweitzer BC, et al. Synaptopathies: synaptic dysfunction in neurological disorders - A review from students to students. *J Neurochem*. 2016;138(6):785–805. https://doi.org/10.1111/jnc.13713
2. Coleman P, Federoff H, Kurlan R. A focus on the synapse for neuroprotection in Alzheimer disease and other dementias. *Neurology*. 2004;63(7):1155–1162. https://doi.org/10.1212/01.WNL.0000140626.48118.0A
3. SCHEFF SW, PRICE DA. Synaptic density in the inner molecular layer of the hippocampal dentate gyrus in Alzheimer disease. *J Neuropathol Exp Neurol*. 1998;57(12):1146–1153. https://doi.org/10.1097/00005072-199812000-00006
4. Scheff SW, DeKosky ST, Price DA. Quantitative assessment of cortical synaptic density in Alzheimer's disease. *Neurobiol Aging*. 1990;11(1):29–37. https://doi.org/10.1016/0197-4580(90)90059-9
5. Scheff SW, Price DA. Synapse loss in the temporal lobe in Alzheimer's disease. *Ann Neurol*. 1993;33(2):190–199. https://doi.org/10.1002/ana.410330209
6. Palop JJ, Mucke L. Amyloid-B-induced neuronal dysfunction in Alzheimer's disease: from synapses toward neural networks. *Nat Neurosci*. 2010;13(7):812–818. https://doi.org/10.1038/nn.2583
7. Spires-Jones TL, Hyman BT. The intersection of amyloid beta and tau at synapses in Alzheimer's disease. *Neuron*. 2014;82(4):756–771. https://doi.org/10.1016/j.neuron.2014.05.004
8. Hong S, Beja-Glasser VF, Nfonoyim BM, et al. Complement and microglia mediate early synapse loss in Alzheimer mouse models. *Science (80-)*. 2016;352(6286):712–716. https://doi.org/10.1126/science.aad8373
9. Rajendran L, Paolicelli RC. Microglia-mediated synapse loss in Alzheimer's disease. *J Neurosci*. 2018;38(12):2911–2919. https://doi.org/10.1523/JNEUROSCI.1136-17.2017
10. Forner S, Baglietto-Vargas D, Martini AC, Trujillo-Estrada L, LaFerla FM. Synaptic impairment in Alzheimer's disease: a dysregulated symphony. *Trends Neurosci*. 2017;40(6):347–357. https://doi.org/10.1016/j.tins.2017.04.002
11. Colom-Cadena M, Spires-Jones T, Zetterberg H, et al. The clinical promise of biomarkers of synapse damage or loss in Alzheimer's disease. *Alzheimer's Res Ther*. 2020;12(1):1–12. https://doi.org/10.1186/s13195-020-00588-4
12. Love S, Siew LK, Dawbarn D, Wilcock GK, Ben-Shlomo Y, SJ Allen. Premorbid effects of APOE on synaptic proteins in human temporal neocortex. *Neurobiol Aging*. 2006;27(6):797–803. https://doi.org/10.1016/j.neurobiolaging.2005.04.008
13. Boros BD, Greathouse KM, Gentry EG, et al. Dendritic spines provide cognitive resilience against Alzheimer's disease. *Ann Neurol*. 2017;82(4):602–614. https://doi.org/10.1002/ana.25049
14. Wilde MC, Overk CR, Sijben JW, Masliah E. Meta-analysis of synaptic pathology in Alzheimer's disease reveals selective molecular vesicular machinery vulnerability. *Alzheimer's Dement*. 2016;12(6):633–644. https://doi.org/10.1016/j.jalz.2015.12.005
15. Davidsson P, Blennow K. Neurochemical dissection of synaptic pathology in Alzheimer's disease. *Int Psychogeriatrics*. 1998;10(1):11–23. https://doi.org/10.1017/S1041610298005110
16. Bogdanovic N, Davidsson P, Volkmann I, Winblad B, Blennow K. Growth-associated protein GAP-43 in the frontal cortex and in the hippocampus in Alzheimer's disease: an immunohistochemical and quantitative study. *J Neural Transm*. 2000;107(4):463–478. https://doi.org/10.1007/s007020070088
17. Sandelius Å, Portelius E, Källén Å, et al. Elevated CSF GAP-43 is Alzheimer's disease specific and associated with tau and amyloid pathology. *Alzheimer's Dement*. 2019;15(1):55–64. https://doi.org/10.1016/j.jalz.2018.08.006
18. Milà-Alomà M, Brinkmalm A, Ashton NJ, et al. CSF synaptic biomarkers in the preclinical stage of Alzheimer disease and their association with MRI and PET. *Neurology*. 2021;97(21):e2065–e2078. https://doi.org/10.1212/WNL.0000000000012853
19. Tible M, Sandelius Å, Höglund K, et al. Dissection of synaptic pathways through the CSF biomarkers for predicting Alzheimer disease. *Neurology*. 2020;95(8):e953–e961. https://doi.org/10.1212/WNL.0000000000010131
20. Hansson O, Seibyl J, Stomrud E, et al. CSF biomarkers of Alzheimer's disease concord with amyloid-β PET and predict clinical progression: a study of fully automated immunoassays in BioFINDER and ADNI cohorts. *Alzheimer's Dement*. 2018;14(11):1470–1481. https://doi.org/10.1016/j.jalz.2018.01.010
21. Desikan RS, Ségonne F, Fischl B, et al. An automated labeling system for subdividing the human cerebral cortex on MRI scans into gyral based regions of interest. *Neuroimage*. 2006;31(3):968–980. https://doi.org/10.1016/j.neuroimage.2006.01.021
22. Landau SM, Fero A, Baker SL, et al. Measurement of longitudinal β-amyloid change with 18 F-florbetapir PET and standardized uptake value ratios. *J Nucl Med*. 2015;56(4):567–574. https://doi.org/10.2967/jnumed.114.148981
23. Landau SM, Mintun MA, Joshi AD, et al. Amyloid deposition, hypometabolism, and longitudinal cognitive decline. *Ann Neurol*. 2012;72(4):578–586. https://doi.org/10.1002/ana.23650
24. Jack CR, Knopman DS, Weigand SD, et al. An operational approach to National Institute on Aging-Alzheimer's Association criteria for preclinical Alzheimer disease. *Ann Neurol*. 2012;71(6):765–775. https://doi.org/10.1002/ana.22628
25. Guo T, Korman D, Baker SL, Landau SM, Jagust WJ. Longitudinal cognitive and biomarker measurements support a unidirectional pathway in Alzheimer's disease pathophysiology. *Biol Psychiatry*. 2021;89(8):786–794. https://doi.org/10.1016/j.biopsych.2020.06.029
26. Jack CR, Wiste HJ, Weigand SD, et al. Defining imaging biomarker cut points for brain aging and Alzheimer's disease. *Alzheimer's Demen*. 2017;13(3):205–216. https://doi.org/10.1016/j.jalz.2016.08.005
27. Schindler SE, Gray JD, Gordon BA, et al. Cerebrospinal fluid biomarkers measured by Elecsys assays compared to amyloid imaging. *Alzheimer's Dement*. 2018;14(11):1460–1469. https://doi.org/10.1016/j.jalz.2018.01.013
28. Bilgel M, An Y, Helphrey J, et al. Effects of amyloid pathology and neurodegeneration on cognitive change in cognitively normal adults. *Brain*. 2018:1–11. https://doi.org/10.1093/brain/awy150. June).
29. Donohue MC, Sperling RA, Salmon DP, et al. The preclinical Alzheimer cognitive composite: measuring amyloid-related decline. *JAMA Neurol*. 2014;71(8):961–970. https://doi.org/10.1001/jamaneurol.2014.803
30. Mattsson-Carlgren N, Andersson E, Janelidze S, et al. Aβ deposition is associated with increases in soluble and phosphorylated tau that precede a positive Tau PET in Alzheimer's disease. *Sci Adv*. 2020;6(16):eaaz2387. https://doi.org/10.1126/sciadv.aaz2387
31. Pereira JB, Janelidze S, Ossenkoppele R, et al. Untangling the association of amyloid-β and tau with synaptic and axonal loss in Alzheimer's disease. *Brain*. 2021;144(1):310–324. https://doi.org/10.1093/brain/awaa395

32. Smith R, Wibom M, Pawlik D, Englund E, Hansson O. Correlation of in Vivo [18 F]Flortaucipir with Postmortem Alzheimer Disease Tau Pathology. *JAMA Neurol*. 2019;76(3):310–317. https://doi.org/10.1001/jamaneurol.2018.3692
33. Barthélemy NR, Li Y, Joseph-Mathurin N, et al. A soluble phosphorylated tau signature links tau, amyloid and the evolution of stages of dominantly inherited Alzheimer's disease. *Nat Med*. 2020;26(3):398–407. https://doi.org/10.1038/s41591-020-0781-z
34. Jack CR, Knopman DS, Jagust WJ, et al. Tracking pathophysiological processes in Alzheimer's disease: an updated hypothetical model of dynamic biomarkers. *Lancet Neurol*. 2013;12(2):207–216. https://doi.org/10.1016/S1474-4422(12)70291-0
35. Sjögren M, Davidsson P, Gottfries J, et al. The cerebrospinal fluid levels of Tau, growth-associated protein-43 and soluble amyloid precursor protein correlate in Alzheimer's disease, reflecting a common pathophysiological process. *Dement Geriatr Cogn Disord*. 2001;12(4):257–264. https://doi.org/10.1159/000051268
36. Remnestål J, Just D, Mitsios N, et al. CSF profiling of the human brain enriched proteome reveals associations of neuromodulin and neurogranin to Alzheimer's disease. *PROTEOMICS – Clin Appl*. 2016;10(12):1242–1253. https://doi.org/10.1002/prca.201500150
37. Bergström S, Remnestål J, Yousef J, et al. Multi-cohort profiling reveals elevated CSF levels of brain-enriched proteins in Alzheimer's disease. *Ann Clin Transl Neurol*. 2021;8(7):1456–1470. https://doi.org/10.1002/acn3.51402
38. Allegra Mascaro AL, Cesare P, Sacconi L, et al. In vivo single branch axotomy induces GAP-43-dependent sprouting and synaptic remodeling in cerebellar cortex. *Proc Natl Acad Sci*. 2013;110(26):10824–10829. https://doi.org/10.1073/pnas.1219256110
39. Tedeschi A, Nguyen T, Puttagunta R, Gaub P, Di GiovanniS. A p53-CBP/p300 transcription module is required for GAP-43 expression, axon outgrowth, and regeneration. *Cell Death Differ*. 2009;16(4):543–554. https://doi.org/10.1038/cdd.2008.175
40. Schreyer DJ, Skene JHP. Injury-associated induction of GAP-43 expression displays axon branch specificity in rat dorsal root ganglion neurons. *J Neurobiol*. 1993;24(7):959–970. https://doi.org/10.1002/neu.480240709
41. Domínguez-álvaro M, Montero-Crespo M, Blazquez-Llorca L, Insausti R, DeFelipe J, Alonso-Nanclares L. Three-dimensional analysis of synapses in the transentorhinal cortex of Alzheimer's disease patients. *Acta Neuropathol Commun*. 2018;6(1):1–15. https://doi.org/10.1186/s40478-018-0520-6
42. Arendt T. Synaptic degeneration in Alzheimer's disease. *Acta Neuropathol*. 2009;118(1):167–179. https://doi.org/10.1007/s00401-009-0536-x
43. Martínez-Serra R, Alonso-Nanclares L, Cho K, Giese KP. Emerging insights into synapse dysregulation in Alzheimer's disease. *Brain Commun*. 2022;4(2):1–11. https://doi.org/10.1093/braincomms/fcac083
44. Lleó A, Núñez-Llaves R, Alcolea D, et al. Changes in synaptic proteins precede neurodegeneration markers in preclinical Alzheimer's disease cerebrospinal fluid*. *Mol Cell Proteomics*. 2019;18(3):546–560. https://doi.org/10.1074/mcp.RA118.001290
45. Yoshiyama Y, Higuchi M, Zhang B, et al. Synapse loss and microglial activation precede tangles in a P301S tauopathy mouse model. *Neuron*. 2007;53(3):337–351. https://doi.org/10.1016/j.neuron.2007.01.010
46. Selkoe DennisJ. Alzheimer's disease is a synaptic failure. *Science (80-)*. 2002;298(5594):789–791.
47. Sheng M, Sabatini BL, Südhof TC. Synapses and Alzheimer's disease. *Cold Spring Harb Perspect Biol*. 2012;4(5). https://doi.org/10.1101/cshperspect.a005777
48. Brinkmalm A, Brinkmalm G, Honer WG, et al. SNAP-25 is a promising novel cerebrospinal fluid biomarker for synapse degeneration in Alzheimer's disease. *Mol Neurodegener*. 2014;9(1):53. https://doi.org/10.1186/1750-1326-9-53
49. Öhrfelt A, Brinkmalm A, Dumurgier J, et al. The pre-synaptic vesicle protein synaptotagmin is a novel biomarker for Alzheimer's disease. *Alzheimer's Res Ther*. 2016;8(1):1–10. https://doi.org/10.1186/s13195-016-0208-8
50. Kvartsberg H, Duits FH, Ingelsson M, et al. Cerebrospinal fluid levels of the synaptic protein neurogranin correlates with cognitive decline in prodromal Alzheimer's disease. *Alzheimer's Dement*. 2015;11(10):1180–1190. https://doi.org/10.1016/j.jalz.2014.10.009

SUPPORTING INFORMATION

Additional supporting information can be found online in the Supporting Information section at the end of this article.

How to cite this article: Lana G, Li A, Liu Z, Ma S, Guo T; for the Alzheimer's Disease Neuroimaging Initiative. Presynaptic membrane protein dysfunction occurs prior to neurodegeneration and predicts faster cognitive decline. *Alzheimer's Dement*. 2022;1-12. https://doi.org/10.1002/alz.12890